ChemComm

COMMUNICATION

View Article Online
View Journal | View Issue

Cite this: *Chem. Commun.*, 2024, **60**, 14395

Received 3rd October 2024,
Accepted 11th November 2024

DOI: 10.1039/d4cc05208k

rsc.li/chemcomm

Tuneable sulfonated hypercrosslinked polymers for selective esterification: insights into performance and stability†

Paul Schweng, [ac] Dorian Guerin-Faucheur,[a] Freddy Kleitz *[b] and Robert T. Woodward *[a]

We report sulfonated hypercrosslinked polymers (SHCPs) as heterogeneous catalysts for the selective esterification of hexanoic acid with benzyl alcohol. The SHCPs demonstrate tuneable catalytic activity and selectivity, outperforming conventional acid catalysts. We also explore detrimental structural changes over multiple cycles, providing insights for optimising long-term catalyst performance.

Increasing socio-economic and environmental pressures are driving a shift toward sustainable practices in the chemical industry. The development of reusable and highly selective catalysts is a key principle of green chemistry, prioritising the minimisation of waste. Effective heterogeneous catalysts that embody these principles can be realised through the immobilisation of catalytically active functionalities onto inert, insoluble scaffolds. Heterogeneous catalysts offer several advantages over their homogeneous counterparts, including straightforward separation from reactants and products, ease of recycling, and potential use in continuous flow processes.[1] Despite these benefits, the application of heterogeneous catalysts in industry is often limited due to high costs, reduced catalytic activities, or poor stabilities.[2] Additionally, the anchoring of catalytic sites to inert scaffolds can lead to changes in their microenvironment, reducing accessibility and/or activity. For heterogeneous catalysts to be effective, they must be cost-efficient, feature dense and accessible active sites, and be applicable to a wide range of catalytic transformations.

Acidic inorganic and organic nanomaterials, including zeolites,[3] mesoporous organosilicas,[4] metal–organic frameworks (MOFs),[5] and organic ion-exchange resins[6,7] have emerged as promising alternatives to homogeneous acid catalysts. However, these classes of materials each come with a unique set of challenges and limitations that restrict their use in industry. The inherent microporosity of zeolites constricts the accessibility of active sites, resulting in mass transfer limitations and slow conversion,[8] while the synthesis of mesoporous silicas often requires several processing steps, including template removal, driving up costs. Many MOFs exhibit poor thermal- and water stability, rendering them unsuitable for a range of catalytic applications.[9] Commercial organic ion-exchange resins, such as Amberlyst-15, although highly acidic, are limited by low surface areas.[10]

Porous organic polymers offer numerous advantages for heterogeneous catalysis, including general chemical inertness, thermal stability, broad pore size distributions for effective mass transfer, and low-densities.[11] Hypercrosslinked polymers (HCP) are a subclass of porous organic polymer comprising densely crosslinked amorphous networks produced using Friedel–Crafts chemistry.[12] An extensive array of synthetic pathways to HCPs offer broad chemical and textural design, permitting the development of HCPs for various applications including gas storage and separation,[13,14] energy storage,[15,16] and water remediation.[17,18] In 2022, we reported a one-pot route to sulfonated hypercrosslinked polymer (SHCP) acid catalysts that allowed for the tuning of active site densities and pore architecture.[19] A library of SHCPs was applied to the acid-catalysed hydrolysis of cyclohexyl acetate to cyclohexanone, where it was found that catalyst amphiphilicity was crucial for optimal substrate conversion in the two-phase reaction.

Esterification plays a key role in industry for the production of paints,[20] varnishes,[21] perfumes,[22] pharmaceuticals[23] and biodiesel. Acid-catalysed esterification reactions typically yield the corresponding ether as a byproduct due to the dehydrative coupling of two alcohol molecules. Herein, we employ SHCPs

[a] *Institute of Materials Chemistry and Research, Faculty of Chemistry, University of Vienna, Währinger Straße 42, 1090, Vienna, Austria. E-mail: robert.woodward@univie.ac.at*
[b] *Department of Functional Materials and Catalysis, Faculty of Chemistry, University of Vienna, Währinger Straße 42, 1090 Vienna, Austria. E-mail: freddy.kleitz@univie.ac.at*
[c] *Vienna Doctoral School in Chemistry, University of Vienna, Währinger Straße 42, 1090, Vienna, Austria*

† Electronic supplementary information (ESI) available. See DOI: https://doi.org/10.1039/d4cc05208k

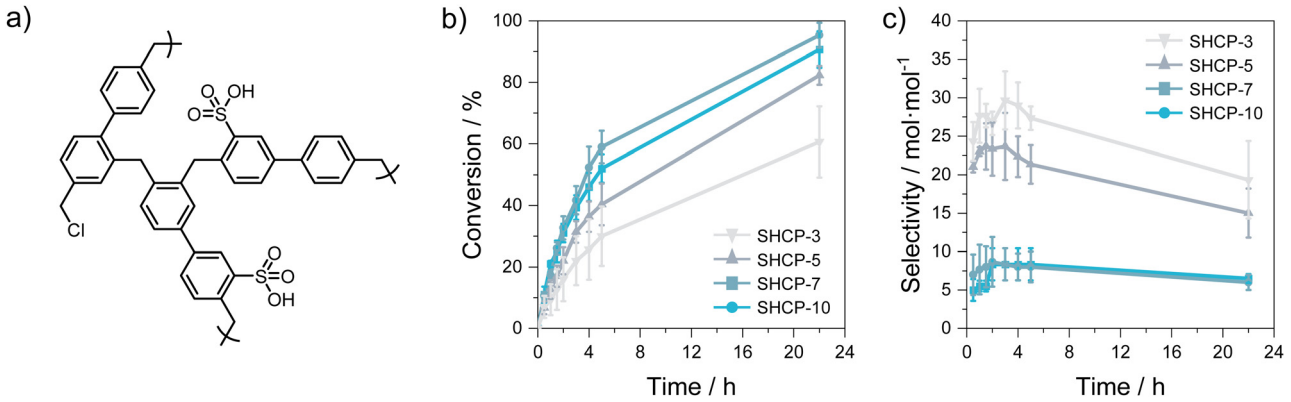

Fig. 1 (a) Representative SHCP structure. (b) Conversion of benzyl alcohol over time, and (c) selectivity toward the desired ester product over the ether by-product upon esterification using SHCP-3 (light grey), SHCP-5 (dark grey), SHCP-7 (grey-blue), and SHCP-10 (blue). Data are provided as mean ± standard deviation (n = 3).

as acid catalysts for the esterification of hexanoic acid with benzyl alcohol, a model reaction used to probe the selectivity and efficiency of acid catalysts. The tuneability of SHCPs allows us to modify their acid-site densities, pore volumes, and surface areas, offering a tailored approach to catalyst design for esterification. By evaluating the catalytic performance of systematically varied SHCPs, we seek to identify key catalyst properties for selective esterification.

We synthesised four SHCPs with varying sulfonation densities following our previous report (representative SHCP structure shown in Fig. 1a).[19] In brief, networks SHCP-3, SHCP-5, SHCP-7, and SHCP-10 were prepared using chlorosulfonic acid as a dual catalyst and sulfonation agent in the self-condensation and sulfonation of 4,4′-bis(chloromethyl)-1,1′-biphenyl. Network nomenclature was retained from our previous research.[19] The successful formation of SHCPs was confirmed by extensive chemical and physical characterisation and agrees well with previous work (see Section S2 of the ESI†).[14,19] Higher sulfonation densities led to a decrease in V_{Tot}, while V_{Micro} remained relatively unchanged, suggesting that sulfonation predominantly occurred within more accessible meso/macropores. Key network data including sulfonate content, Brunauer–Emmett–Teller (BET) specific surface area, micropore volume (V_{Micro}), and total pore volume (V_{Tot}) are provided in Table 1.

Table 1 Sulfonate content and porous properties of SHCPs, including BET surface area, micropore volume V_{Micro}, and total pore volume V_{Tot}. Data are provided as mean ± standard deviation (n = 3)

Network	Catalyst: monomer	Sulfonate content (mmol g^{-1})[a]	BET surface area (m^2 g^{-1})[b]	V_{Micro} (cm^3 g^{-1})[b]	V_{Tot} (cm^3 g^{-1})[b]
SHCP-3	0.5	1.26 ± 0.16	1093 ± 228	0.16 ± 0.04	0.82 ± 0.27
SHCP-5	1.0	2.19 ± 0.31	954 ± 59	0.21 ± 0.02	0.58 ± 0.02
SHCP-7	2.0	3.40 ± 0.42	777 ± 34	0.17 ± 0.02	0.49 ± 0.09
SHCP-10	4.0	4.44 ± 0.23	645 ± 48	0.17 ± 0.02	0.34 ± 0.02

[a] Determined using XPS analysis. [b] Derived from N_2 sorption isotherms recorded at 77 K.

SHCPs with varied chemical and textural properties were applied to the esterification of hexanoic acid with benzyl alcohol (reaction scheme shown in Fig. S1, ESI†), to investigate their efficiency with respect to both conversion and selectivity. Briefly, SHCP was added to a mixture containing both reactants in dry toluene, which was heated at 75 °C in a nitrogen atmosphere for 22 h. The reaction was sampled at regular intervals, diluted in ethyl acetate, and analysed using gas chromatography-mass spectrometry (GC-MS). Benzyl alcohol conversions over time are plotted in Fig. 1b (corresponding GC traces and numerical data are shown in Fig. S6 and Table S2 (ESI†), respectively). Network SHCP-3 displayed the lowest catalytic activity and the highest standard deviation across all samples, reaching 61 ± 12% conversion after 22 h. The relatively poor catalytic activity of SHCP-3 is due to its low sulfonation density. The more acidic SHCP-5 gave benzyl alcohol conversions of 82 ± 3% after 22 h, while SHCP-7 and SHCP-10 both achieved a substrate conversion of ≥90%, exceeding the performance of both the commercial resin Amberlyst-15 and homogeneous (liquid) H_2SO_4.[24] Control experiments utilising a non-acidic hypercrosslinked polymer equivalent showed negligible conversion after 22 h (Fig. S7, ESI†), confirming the role of the acidic sulfonate moieties. Achieving high sulfonation densities did not appear crucial for catalyst performance, as the more acidic SHCP-10 displayed similar conversion rates to SHCP-7, in which catalytic conversion reached a maximum of 95 ± 4%. The elevated activity in SHCP-7 may be attributed to the higher surface area and improved mesopore/macropore content, resulting in greater accessibility to catalytic sites.

The two polymers with the highest acidity and conversion rates, SHCP-7 and SHCP-10, exhibited the lowest selectivity for the ester product, with values of 6 ± 1 and 7 ± 1 mol mol^{-1} after 22 h, respectively (Fig. 1c and Table S3, ESI†). It is noteworthy that, although these selectivities are not optimal for industrial application, they are superior to Amberlyst-15.[24] Conversely, the polymers with lower sulfonation densities, SHCP-3 and SHCP-5, exhibited significantly higher selectivities

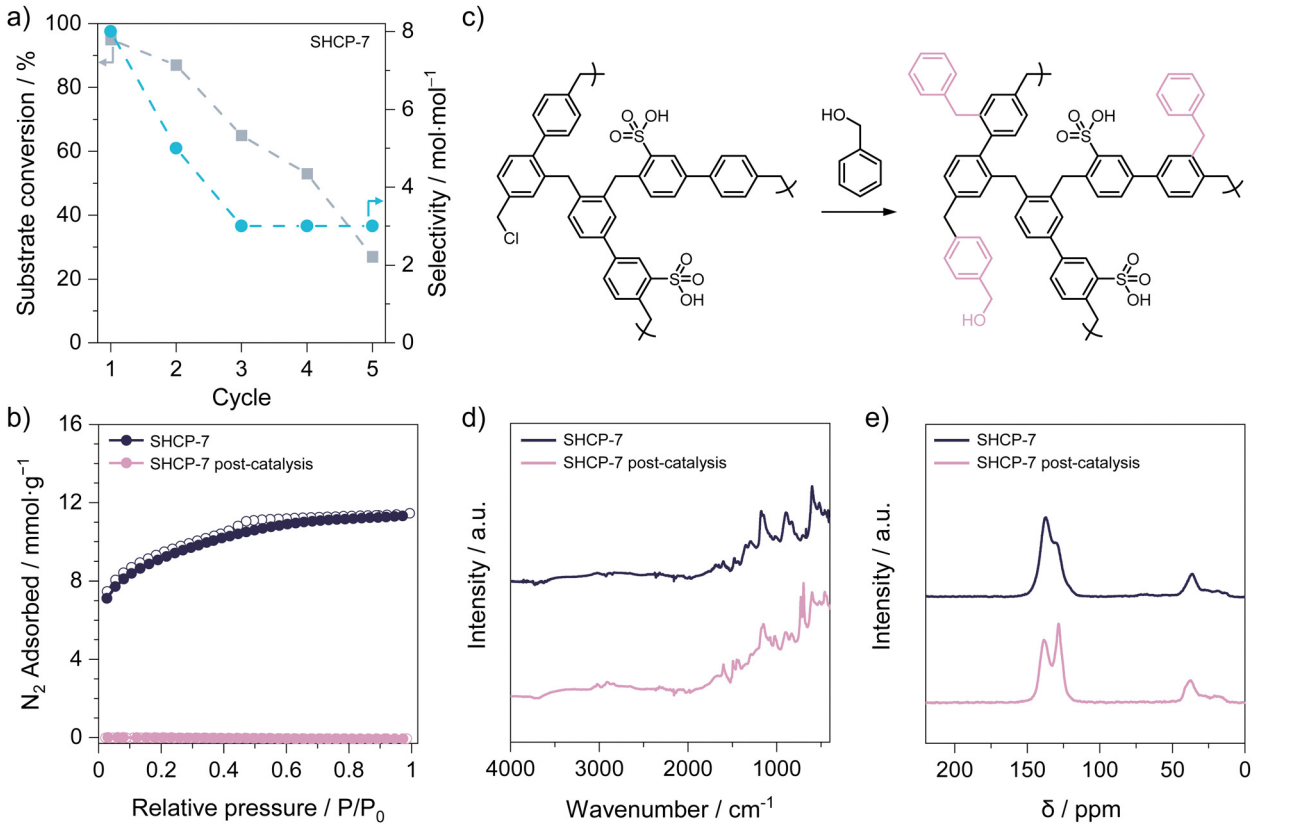

Fig. 2 (a) Catalytic efficiency of SHCP-7 across five cycles, showing benzyl alcohol conversion and ester/ether selectivity. (b) N_2 sorption–desorption isotherms of SHCP-7 (dark blue) before and after (pink) cycling, measured at −196 °C. (c) Scheme of benzyl alcohol condensation onto an SHCP, the proposed cause of gradual catalytic decline. (d) FTIR spectra and (e) ^{13}C CP/MAS ssNMR of SHCP-7 before and after cycling.

after three hours, reaching 24 ± 4 and 30 ± 4, respectively, comparable to that of a homogeneous sulfuric acid catalyst[24] but inferior to sulfonated polymer networks with columnar hexagonal pore structures.[25] The performance of SHCP catalysts for this esterification is compared with examples from the literature in Table S4 (ESI†). Considering the lower conversion rates of SHCP-3 and SHCP-5, their improved selectivity indicates the initial slow formation of the desired ester product, followed by ether production. When using the more acidic SHCP-7 and SHCP-10, the reaction proceeds faster, and thus also leads to the formation of more ether product. Interestingly, the selectivity of all samples decreased after 22 h reaction time, again indicating elevated ether formation with time.

To assess cycling stability, a total of five consecutive catalysis experiments were conducted utilising SHCP-7, given that this displayed the highest benzyl alcohol conversion rate (Section S3 of the ESI†). The catalytic efficiency of SHCP-7 exhibited a gradual decline across the five cycles (Fig. 2a and Table S5, ESI†), with the initial conversion of 95 ± 4% in the first cycle decreasing to just 27% in the fifth. The drop in catalytic efficiency is in contrast to the repeated hydrolysis of cyclohexyl acetate to cyclohexanol using SHCP-10, where no measurable changes were observed upon cycling.[19] Attempts to regenerate the catalysts by washing with 1 M HCl acid or thermal treatment at 150 °C for 1 h were unsuccessful. Wolska *et al.*[26] reported a decrease in catalytic activity for similar SHCPs in the esterification of acetic acid with various alcohols. There, the decline was attributed to leaching of sulfonic acid moieties over time. To assess the catalyst stability and potential leaching phenomena, we reanalysed SHCP-7 after cycling. Post-cycling, N_2 sorption isotherms of SHCP-7 (Fig. 2b) showed an almost complete pore structure collapse, resulting in a BET surface area reduction from 777 ± 34 to just 1 m^2 g^{-1}, *i.e.* non-porous. X-ray photoelectron spectroscopy (Table S6, ESI†) showed a reduction in both sulfur and chlorine content after recycling, as well as an increase in oxygen and carbon content. The changes in elemental composition upon recycling suggest the incorporation of benzyl alcohol *via* condensation reactions, *i.e.* conversion of both residual chloromethyl groups of the SHCP and hydroxymethyl groups of the benzyl alcohol into additional methylene bridges (Fig. 2c). Fourier transform infrared spectroscopy (Fig. 2d) showed the emergence of bands at 726 cm^{-1} and 698 cm^{-1}, assigned to monosubstituted aromatic rings, in agreement with the increased carbon content measured *via* XPS. Further analysis of the recovered SHCP-7 using ^{13}C cross-polarisation/magic angle spinning solid-state NMR (CP/MAS ssNMR, Fig. 2e) revealed an increase in the ratio of unsubstituted to substituted aromatic carbon, in agreement with the addition of mono- and disubstituted aromatic rings. Thermogravimetric analysis of recovered SHCP-7 (Fig. S9, ESI†)

revealed a reduced residual water content, indicative of diminished hydrophilicity. Luo *et al.* reported the self-condensation of benzyl alcohol using a Lewis acid catalyst for the formation of a hypercrosslinked polymer.[27] With this in mind, considering the analysis of the recovered SHCP-7, it is proposed that benzyl alcohol molecules are attached to SHCP-7 during the conversion reaction *via* acid-catalysed condensation. The detrimental effect of this attachment is exacerbated with subsequent catalytic cycles, in which the adduct is replenished. In contrast to Wolska *et al.*, who proposed the leaching of sulfonate moieties, our findings indicate that the condensation of benzyl alcohol onto the network gradually dilutes the sulfonate content of the catalyst, reducing acidity, hydrophilicity, and network porosity.

To conclude, we use low-cost and tuneable sulfonated hypercrosslinked polymers in the esterification of hexanoic acid with benzyl alcohol. The importance of high active site densities was underscored by SHCP-7 and SHCP-10, which displayed the highest conversion rates, reaching a maximum of 95 $\pm$ 4% after 22 h, higher than that of sulfuric acid and the commercial ion-exchange resin Amberlyst-15. Lower sulfonate concentrations in SHCPs led to decreased catalytic activity yet significantly improved selectivities, achieving values of up to 30 $\pm$ 4, underlining the potential for further catalyst optimisation. Finally, we put forth a mechanism for the poor cycling stability of SHCP-7, in which the condensation of benzyl alcohol onto the catalyst surface led to a decline in efficiency.

The authors acknowledge the funding support of the University of Vienna (Austria). We thank Ms Gaeun Park for her assistance with recycling experiments. We also thank EPF Graduate School of Engineering (Montpellier, France) for supporting D. G.-F. during his internship, as well as the NMR Centre (University of Vienna) for assistance with ssNMR.

Data availability

The data supporting this article have been included as part of the ESI.†

Conflicts of interest

There are no conflicts to declare.

References

1 J. Chen, Y. Gao, S. Zuo, H. Mao, X. Li, W. Liu, C. Yao and H. Gui, *Langmuir*, 2024, **40**, 3024–3034.
2 S. Hübner, J. G. de Vries and V. Farina, *Adv. Synth. Catal.*, 2016, **358**, 3–25.
3 J. Bao, Q. Yang, S. Zeng, X. Sang, W. Zhai and H. Nie, *Microporous Mesoporous Mater.*, 2022, **337**, 111897.
4 M. Choi, F. Kleitz, D. Liu, H. Y. Lee, W.-S. Ahn and R. Ryoo, *J. Am. Chem. Soc.*, 2005, **127**, 1924–1932.
5 C. A. Trickett, T. M. Osborn Popp, J. Su, C. Yan, J. Weisberg, A. Huq, P. Urban, J. Jiang, M. J. Kalmutzki, Q. Liu, J. Baek, M. P. Head-Gordon, G. A. Somorjai, J. A. Reimer and O. M. Yaghi, *Nat. Chem.*, 2019, **11**, 170–176.
6 Y. Hu, H. Li, D. Wu, L. Li, C. Hu and L. Zhu, *Catal. Today*, 2024, **442**, 114939.
7 N. Boz, N. Degirmenbasi and D. M. Kalyon, *Appl. Catal., B*, 2015, **165**, 723–730.
8 Y. Wei, T. E. Parmentier, K. P. de Jong and J. Zečević, *Chem. Soc. Rev.*, 2015, **44**, 7234–7261.
9 N. C. Burtch, H. Jasuja and K. S. Walton, *Chem. Rev.*, 2014, **114**, 10575–10612.
10 M. A. Harmer and Q. Sun, *Appl. Catal., A*, 2001, **221**, 45–62.
11 Y. Gu, S. U. Son, T. Li and B. Tan, *Adv. Funct. Mater.*, 2021, **31**, 2008265.
12 L. Tan and B. Tan, *Chem. Soc. Rev.*, 2017, **46**, 3322–3356.
13 C. Wood, B. Tan, A. Trewin, F. Su, M. Rosseinsky, D. Bradshaw, Y. Sun, L. Zhou and A. Cooper, *Adv. Mater.*, 2008, **20**, 1916–1921.
14 P. Schweng, F. Mayer, D. Galehdari, K. Weiland and R. T. Woodward, *Small*, 2023, **19**, 2304562.
15 O. Hubert, N. Todorovic, L. M. Rojas González, E. Costagliola, A. Blocher, A. Mautner, R. T. Woodward and A. Bismarck, *Compos. Sci. Technol.*, 2023, **242**, 110152.
16 R. Vinodh, C. V. V. M. Gopi, V. G. R. Kummara, R. Atchudan, T. Ahamad, S. Sambasivam, M. Yi, I. M. Obaidat and H.-J. Kim, *J. Energy Storage*, 2020, **32**, 101831.
17 F. Mayer, P. Schweng, S. Braeuer, S. Hummer, G. Koellensperger, A. Mautner, R. Woodward and A. Bismarck, *Small Sci.*, 2024, **4**, 2400182.
18 A. M. James, S. Harding, T. Robshaw, N. Bramall, M. D. Ogden and R. Dawson, *ACS Appl. Mater. Interfaces*, 2019, **11**, 22464–22473.
19 A. Blocher, F. Mayer, P. Schweng, T. M. Tikovits, N. Yousefi and R. T. Woodward, *Mater. Adv.*, 2022, **3**, 6335–6342.
20 S. M. Mirabedini, F. Zareanshahraki and V. Mannari, *Prog. Org. Coat.*, 2020, **139**, 105454.
21 V. Benessere, M. E. Cucciolito, A. De Santis, M. Di Serio, R. Esposito, M. Melchiorre, F. Nugnes, L. Paduano and F. Ruffo, *J. Am. Oil Chem. Soc.*, 2019, **96**, 443–451.
22 A. G. A. Sá, A. C. de Meneses, P. H. H. de Araújo and D. de Oliveira, *Trends Food Sci. Technol.*, 2017, **69**, 95–105.
23 H. C. Arca, L. I. Mosquera-Giraldo, V. Bi, D. Xu, L. S. Taylor and K. J. Edgar, *Biomacromolecules*, 2018, **19**, 2351–2376.
24 S. Bilodeau, J. Florek and F. Kleitz, *Chem. Ing. Tech.*, 2021, **93**, 916–928.
25 Y. Xu, W. Gu and D. L. Gin, *J. Am. Chem. Soc.*, 2004, **126**, 1616–1617.
26 J. Wolska and L. Wolski, *Arab. J. Chem.*, 2024, **17**, 105600.
27 Y. Luo, S. Zhang, Y. Ma, W. Wang and B. Tan, *Polym. Chem.*, 2013, **4**, 1126–1131.

